FACTA UNIVERSITATIS (NIŠ)
SER.: ELEC. ENERG. vol. 20, no. 1, Mart 2007, 1-8

Computation and Measurement of Low Frequency Magnetic Field Near Thin-Wire Structures

Sonja Filiposka, Vesna Arnautovski-Toševa, and Leonid Grčev

Abstract: Magnetic fields in residential and occupational environments attract attention due to concerns of health risks. This paper describes comparison of two simple numerical procedures for computation of magnetic fields due to sources typical for residential environment which can be also used for teaching purposes. The methods are confirmed with the results obtained by analytical closed form solution and experimental laboratory measurements.

Keywords: Low frequency magnetic fields, method of moments, Biot-Savart law, teaching example measurements.

1 Introduction

The biological effects of electromagnetic fields on human health have been a concern for decades [1]. Recent classification of low frequency magnetic fields in residential and working environments as possible human carcinogen by IARC [2] reflects continuing efforts by numerous ongoing experimental research studies to determine the risk in practical situations.

In a number of cases in the residential environments the magnetic field is created by conductors that usually conform to thin-wire approximation, i.e. they might be considered as consisted of a network of straight segments with lengths much greater than their radiuses. Consequently, only the line currents along axes of such conductors might be considered, which allows more simplified modeling. A complex technique for computation of fields due to residential wiring based on the

Manuscript received June 22, 2005. An earlier version of this paper was presented at seventh International Conference on Applied Electromagnetics ΠΕС 2005, May 23-25, 2005, Niš, Serbia.

The authors are with Ss. Cyril and Methodius, Faculty of Electrical Engineering, Karpos II bb, Skopje, Macedonia (e-mails: [filipos, atvesna, lgrcev]@etf.ukim.edu.mk).

method of moments is described in [3, 4] using the rigorous solution in [5]. However, at low frequencies simpler methods are applicable. The distribution of currents might be obtained by usual power system analysis [6], and fields have to be determined for line current sources.

For the purposes of creating teaching examples the rising need is for simple, yet effective computational methods that can later be compared with real experimental laboratory tests. This paper compares two simple computational procedures, the first one is derived from antenna theory near field computation technique [7], which is applicable at low and high frequencies, and the other for low frequencies based on Biot-Savart law. The numerical results are then compared with laboratory measurements for a simple case of rectangular loop, which is still very often used as a model for more complex situations.

2 Computation of the Magnetic field

2.1 Method of moments

Following the method of moments, the wire is considered as a network of short current segments connected together. Following the thin-wire approximations, the magnetic field $\vec{H}$ produced by line current density $\vec{I}(l)$ along the wire axis is expressed in terms of magnetic vector potential $\vec{A}$ in integral form [1]:

$$\vec{H} = \frac{1}{\mu_0} \nabla \times \vec{A} \tag{1}$$

$$\vec{A} = \mu_0 \int\limits_{axis} \vec{I}(l) \frac{e^{-jkR_m}}{4\pi R_m} \mathrm{d}l \tag{2}$$

where R denotes the distance from the source point on the axis to a field point on the wire surface, and a is the wire radius.

A solution to the above equation is obtained by the well-known moment methods procedures with pulse expansion for current and point matching [8]. Fig.1 shows typical source segment n of length Δl_m with terminal points n^+ and n^-, and its midpoint n.

The calculation of the near magnetic field at arbitrary point m is performed using test segment Δl_m positioned in a desired direction, which leads to the following expression:

$$\vec{A}(m) = \mu_0 \vec{I}(n) \Delta l_n \Psi(n,m) \tag{3}$$

$$\Psi(n,m) = \frac{1}{\Delta l_n} \int\limits_{\Delta l_n} \frac{e^{-jkR_m}}{4\pi R_m} \mathrm{d}l \tag{4}$$

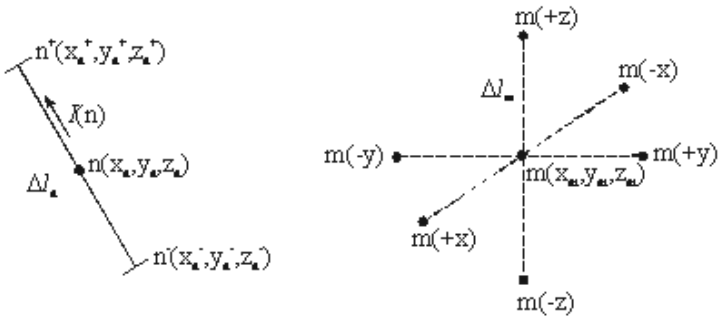

Fig. 1. A view of a source and test current segments in the moment method approach

where R_m is distance from a point on Δl_n to the point m. The direction of the magnetic vector potential $\vec{A}(m)$ is the same with the direction of the source current segment, and can be represented by its Cartesian components

$$\begin{aligned} A_{x,y,z} &= \mu_0 I(n)\Delta l_n \Psi(n,m)\cos\alpha_{xn,yn,zn} \\ &= \mu_0 I(n)\Delta l_n \Psi_{z,y,z}(n,m) \end{aligned} \tag{5}$$

An approximate solution of the integral in (4) with respect to the distance source-observer is given in [8], which is obtained by expanding the exponential in Maclaurin series

$$\Psi(n,m) = \frac{e^{-jkr}}{4\pi\Delta l_n}\int_{n^-}^{n^+}(\frac{1}{R_m} - jk - \frac{k^2}{2}R_m + \cdots)\mathrm{d}l_n \tag{6}$$

where $k = \omega\sqrt{\varepsilon_0\mu_0}$ is the wave number.

For $n = m$, the two-term integration gives good accuracy

$$\Psi(n,m) \simeq \frac{1}{2\pi\Delta l_n}\log(\frac{\Delta l_n}{a}) - \frac{jk}{4\pi} \tag{7}$$

For $n \neq m$, the crudest approximation is obtained by considering

$$\Psi(n,m) \simeq \frac{e^{-jkR_{mn}}}{4\pi R_{mn}} \tag{8}$$

where R_m is the distance from midpoints n to m. For the quasi-static case it is convenient to consider the following approximation

$$\Psi(n,m) \simeq \frac{1}{4\pi R_{mn}} \tag{9}$$

3 Method Based On Biot-Savart Law

At low frequencies, such as 50 Hz, the magnetic flux density of the field of a complete circuit C carrying a current I may be determined by direct application of the Biot-Savart law [9, 10]. After fictitious segmentation of the circuit into network of current segments as shown on Figure 1, the magnetic flux density of the field at the given point whose position relative to the small element of length $\mathrm{d}l_n$(along the source segment Δl_n) is determined by the position vector is

$$\vec{B} = \sum_n \int_{n^-}^{n^+} \frac{\mu_0}{4\pi} \frac{I \mathrm{d}\vec{l}_n \times \vec{r}}{r^3}. \tag{10}$$

For simple circuit geometry the magnetic flux density $\vec{B}$ may be easily determined in closed form by the analytical solution of (15). Thus, the intensity of the magnetic flux in the center of a rectangular frame with dimensions $a \times b$ is

$$B_0 = \frac{2\mu_0 NI}{\pi}\left(\frac{\sin\alpha}{b} + \frac{\sin\beta}{b}\right) \tag{11}$$

where $\tan\alpha = a/b$, $\tan\beta = b/a$. Along the x-axis, the x component of the magnetic flux density is

$$B_x = \frac{2\mu_0 NI}{\pi} \frac{ab}{\sqrt{a^2+b^2+4x^2}}\left(\frac{1}{a^2+4x^2} + \frac{1}{b^2+4x^2}\right) \tag{12}$$

A lot faster, easier and more flexible approach is to calculate the magnetic induction in the vicinity of the observed conductors using superposition of the magnetic inductions obtained for each linear segment of the created model. This means that instead of viewing a small element of length along the source segment, the complete source segment (the rectangular frame in this case) is divided into a minimum number of linear segments. During this operation, each segment is defined with its start and end point coordinates, and the module and phase of the current that flows through the given segment with a direction from the starting towards the end point.

When considering the magnetic induction in a point that lies in the same plane with the observed linear segment which is the origin of this magnetic induction, the following relation of the Bio-Savart law can be used [9].

$$\begin{aligned} B = \int \mathrm{d}B &= \frac{\mu_0}{4\pi}\frac{I}{d}\int_{\theta_1}^{\theta_2} \sin\theta \mathrm{d}\theta \\ &= \frac{\mu_0}{4\pi}\frac{I}{d}(\cos\theta_1 - \cos\theta_2) \end{aligned} \tag{13}$$

where θ_1 is the angle between the radius vector of the calculation point related to the starting point of the linear segment and the radius vector of the linear segment directed according to the current I, θ_2 is the angle between the radius vector of the calculation point related to the end point of the linear segment and the radius vector of the linear segment directed according to the current I, while d is the normal distance from the calculation point to the linear segment.

Using the principles of the method of superposition the x, y and z components of the result magnetic flux density in a given point is obtained as a summation of the components calculated for each distinctive linear segment of the current contour or contours, which were obtained using a coordinate system translation and vector algebra.

This method of computation of the magnetic flux density can be transcribed programmatically and, then, connected to a suitable graphical display program that will allow fast visual observation of the obtained results [10]. The approach is very fitting especially for school examples, since the students only have to give the initial data feed that consists of a list of the observed linear segments. It is also applicable for cases where the exact position of the equipment or conductor contours make the on-field measurements difficult, thus avoiding the constant problem of expensive equipment, as well as for more difficult problems when considering a complex shaped loop.

4 Measurements

The obtained results for the proposed computation method based on the Biot-Savart law and the numerical moment method solution of the magnetic flux density caused by a test rectangular current loop can be compared with the results experimentally determined by measurements. The examined test example is (415 $\times$ 276) mm rectangular current loop with $N = 517$ turns made of fine wire (model 147 S/N 94 magnetic Field generator) product of *Electric Field Measurements* shown on figure 2(a). The measuring scheme and the applied equipment for the magnetic flux density measurements are presented on figure 2(b).

The voltage feeding is performed by $\sim$ 220V, 50Hz voltage generator (1). The current in the rectangular loop (2) is formed by means of the regulating resistor (4) and resistances of 10 kω and 100 kΩ (5) and measured by ampermeter (3). The magnetic flux density measurement is performed by means of the *Electric Field Measurements* EFM 140-3-50 probe-plug connected to digital multimeter METEX M-3800 (6).

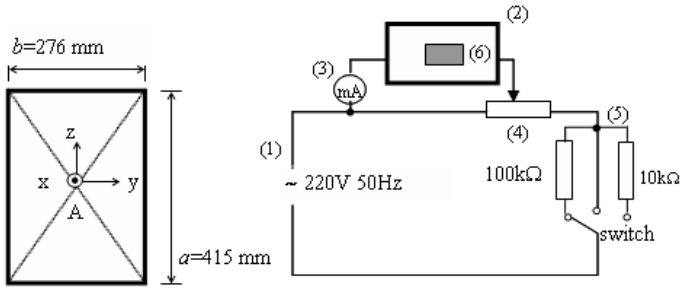

Fig. 2. (a) A test rectangular loop and (b) The measuring scheme

5 Experimental and Numerical Results

The results determined by experiments that will be presented in this section are obtained by series of measurements using various values of the current in the rectangular loop. In Table 1, the comparative values of the magnetic flux density at the origin (point A) obtained by using the both method approaches and measurement are presented: Magnetic Flux Density *x*-component (mG), Current (ma), Analytical (Biot-Savart approach), Computational (Biot-Savart approach), Numerical (Method of moments approach), Experimental.

Table 1. Magnetic flux density at the center of the rectangular loop.

	Magnetic Flux Density *x*-component (mG)			
Current (mA)	Analytical (Bio-Savart Approach)	Comotational (Bio-Savart Approch)	Numerical (Method of moments approach)	Experimental
0.28	5.04	5.04	5.10	5.1
0.56	10.08	10.08	10.09	11.4
0.87	15.66	15.66	15.40	15.9
0.96	17.28	17.28	17.11	17.1
2.64	47.51	47.51	46.8	46.3
5.62	101.14	101.14	100.0	99.1
8.43	151.71	151.71	149.5	144
9.56	172.05	172.05	169.4	165
12.93	232.70	232.70	229.5	228
30.91	556.29	556.29	549.2	550
84.32	1517.51	1517.51	1496	1360
196.71	3540.19	3540.19	3494	3300

Table 2 presents the comparative values of the magnetic flux density at points along the *x*-axis obtained by using the analytical solution of (15), the moment method approach and measurement.

Table 2. The values of magnetic flux density at points along the x-axis.

Current 0.956 mA	Magnetic Flux Density *x*-component (mG)			
Distance along *x*-axis (cm)	Analytical (Bio-Savart Approach)	Comotational (Bio-Savart Approch)	Numerical	Experimental
0	17.21	17.21	17.11	17.1
5	15.23	15.23	15.11	15.0
10	11.23	11.23	11.17	10.8
15	7.65	7.65	7.60	7.0
20	5.13	5.13	5.10	4.4
25	3.49	3.49	3.46	2.9
30	2.42	2.42	2.40	1.9

The results presented in table 1 and table 2 prove that the analytically or numerically determined results are in very good agreement with the measurements taking into account that the magnetic field has three components which makes it very hard to correctly position the probe.

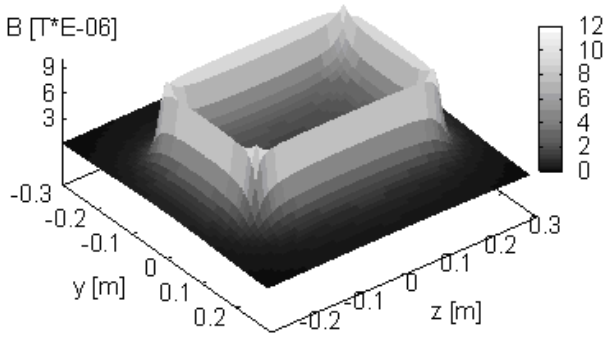

Fig. 3. Spatial distribution of the magnetic flux density in the *yz* plane for $x = 1$ cm and $I = 0.956$ mA

Figure 3 shows the spatial distribution of the magnetic flux in the vicinity of the rectangular frame. The values are obtained using the computational approach based on the Biot-Savart law. This possibility for 2D visualization of the magnetic flux density using this approach has proved as a valuable benefit for educational and professional purposes.

6 Conclusion

In this paper four different approaches to define the magnetic flux intensity in the vicinity of a simple rectangular loop with low frequency current are presented. The

matching results show that the method of moments and the Biot-Savart computational approach based on linearization of the spatial geometry can successfully be used for educational purposes. The second approach is very useful when considering more complex wired structures, while at the same time it allows an easy and fast visualization of the magnetic flux density in the space around the magnetic source.

The computer results are compared with measurements that were performed in laboratory using a test rectangular thin-wire loop and with the analytical solution obtained by a direct application of the Biot-Savart law. It is well known that the moment methods solution is applicable for high frequencies, but this test proves that it is applicable also for low frequencies such as 50 Hz without any modifications. This proves that this powerful method may be directly used for analysis of the low frequency magnetic fields due to wiring in residential and working environments. This may be of interest in studies of the health risk due to low frequency magnetic field.

References

[1] K. R. Foster and a. E. M. L. S. Erdreich, "Weak electromagnetic fields and cancer in the context of risk assessment," *Proc. of the IEEE*, vol. 85, pp. 733–746, May 1997.

[2] International Agency for Research on Cancer, 2002, iARC Monographs. [Online]. Available: http://www.iarc.fr

[3] G. B. Johnson, "Residential field source at power frequencies," in *IEEE International Symposium on Electromagnetic Compatibility*, 1993, pp. 132–137.

[4] F. P. Dawalibi, "Computation of electromagnetic fields produced by electric power lines and residential electrical wiring," *IEEE Trans. on Power Delivery*, vol. 8, pp. 1285–1294, July 1993.

[5] L. Grcev and F. Dawalibi, "An electromagnetic model for transients in grounding systems," *IEEE Trans. on Power Delivery*, vol. 5, no. 4, pp. 1773–1781, Oct. 1990.

[6] D. L. Mader and L. Zafanella, "Network analysis of ground currents in a residential distribution system," *IEEE Trans. on Power Delivery*, vol. 8, pp. 344–350, Jan. 1993.

[7] A. T. Adams, T. E. Baldwin, and D. E. Warren, "Near fields of the thin-wire antennas-computation and experiment," *IEEE Trans. on Electromagnetic Compatibility*, vol. EMC-20, pp. 259–266, Feb. 1978.

[8] R. F. Harrington, *Field Computation by Moment Methods*. IEEE Press, 1992.

[9] I. B. Savalyev, *Physics Volume II Electricity and Magnetism Waves Optics*. Mir Publishers, 1980, (English translation).

[10] S. Filiposka, "Quasi steady state magnetic field calculations in vicinity of complex shaped conductors," in *Int. PhD-seminar Computation of Electromagnetic Fields*, Budva, Serbia & Montenegro, Sept. 2004.